

Dear Reviewers, dear Editor,

We would like to thank again the two Reviewers for the generally positive feedback and constructive criticism on our manuscript.

Below, you can find all comments (in black), our individual responses and changes made to the manuscript (both in green). We hope our responses and changes satisfy the Reviewers.

Kind regards,
Fabian Große

On behalf of all authors

Review #1 by Hagen Radtke

General remarks

The article has a clear scientific objective and is written clearly and concisely. It provides new insights into East China Sea hypoxia.

Unfortunately I see two major shortcomings which need to be clarified before the article can be published. The first one is about the appropriateness of using a simplification of the nutrient tagging method for this application. The second one is about insufficient model validation. If these can be fixed and the authors show that (a) the method is applicable and (b) the model has a sufficient quality in the parameters in question, I would recommend publication of the article.

Reply: Thank you for your generally positive assessment. We believe that the two major points that you raised are addressed in the revision. Please see detailed responses below.

Choice of the tagging method

I see a serious issue with the applied tagging method.

Problem

Your equation (2) presented in line 101 does not describe the element tracing method described in Menesguen et al. (2006) and Radtke et al. (2012), which deviates from the full equation.

[equations removed]

In your 2017 publication ("A Novel Modeling Approach to Quantify the Influence of Nitrogen Inputs on the Oxygen Dynamics of the North Sea") you discussed this problem in a specific paragraph, but you do not state this difference here.

The effect is that in the simplified equation, mixing or advection of the tagged element is always driven by a gradient in the total concentration C_x . So your formulation does not allow a diffusion or advection of a tagged element C_{x_i} against the gradient of the total concentration C_x .

This is especially problematic in this application, where you try to investigate how much oceanic N enters the (N-richer) coastal area. Your simplification prevents this transport. In this way, the contribution of a "local" source is systematically overestimated while that of a

remote source is underestimated. I cannot see why it can be ruled out that this methodological error actually determines the result of your study.

Suggested solution

I suggest a simple experiment to quantify the impact of the simplification. In a first step, you initialize three passive tracers with the concentrations of

- p_1 = riverine N,
- p_2 = non-riverine N and
- p_3 = totalN

at some single time step. Then you run the model for a few years and see how these spread. I expect that your numerical scheme will be linear and $p_1+p_2=p_3$ will be maintained as it should.

Then, initialize two "active elements" (whose spreading is calculated by equation (2)):

- a_1 = riverine N,
- a_2 = non-riverine N.

with the same initial concentrations, using p_3 as their "parent element". Make them practically passive by setting $R_{p_1} = R_{p_2} = 0$. If the simplification error is negligible, a_1 should behave very similar to p_1 and a_2 to p_2 , and you should end up with very similar ratios of non-riverine N to total N in both methods. Then you could present this as a verification that your simplification error is small.

If my expectation is right and the results will show a significant difference, this would mean that you have to apply the full rather than the simplified method for this application.

Reply: Thank you for spotting this. The advection term in our Eq. (2) was written incorrectly and confused the differential term describing the change in the concentration at a location with the discretization of the calculation of the advective transports across the grid cell interfaces. Advection of a labelled tracer is calculated correctly and we corrected Eq. (2) accordingly.

In fact, not only the advection term but also the diffusion term had to be corrected as its previous formulation in Eq. (2) implied that diffusion of a labeled tracer is calculated as the change in concentration of the corresponding non-labeled (i.e. bulk) tracer and the ratio of labelled over non-labeled tracer at location (x,y,z) . However, the discretized diffusion flux across each individual grid cell interface is based on the gradient of the bulk tracer across that interface and the ratio of labeled over non-labeled tracer in the source cell (i.e. the cell in which the bulk tracer concentration is reduced by the diffusion flux across an individual interface).

While we are aware of the point you made that diffusion fluxes of labeled tracers (across individual grid cell interfaces) follow the gradient of the bulk tracer in our approach, we know that numerical diffusion in the MPDATA advection scheme here applied is much higher than turbulent diffusion. Thus, the effect of our simplification is small. This aspect is discussed in the new section 4.1 of the revised manuscript (lines 255-260).

Missing validation

You refer to an existing publication for the model validation. That is not sufficient. Your study relies on the assumption that at least the following is reproduced by the model:

1. lateral nitrogen transport,
2. oxygen consumption rates,
3. hypoxic area extent.

You should then present model validation that proves that the model is capable to do that. I am thinking of

1. DIN observations,
2. benthic chamber lander O₂ fluxes or, if not existent, at least primary production rates as a proxy,
3. observational-based estimates of the hypoxic area.

Reply: We have now included a validation of surface and bottom dissolved inorganic nitrogen (DIN) based on observational data from Gao et al. (2015) in the supplement (Text S3, Figs. S2-S4). A reference to Figs. S2-S4 was included in the model description (line 84) and a discussion of model skill with respect to DIN, sediment oxygen consumption and hypoxic area has been added to the discussion section (part of new Sect. 4.1; lines 227-240). We did not include additional validation of hypoxic area as we consider this redundant with the validation provided in the companion paper by Zhang et al. in this Special Issue (<https://www.biogeosciences-discuss.net/bg-2019-341/>). We refer to this paper where appropriate in the new discussion section 4.1 of the revised manuscript (lines 225, 231).

Specific comments

L38: The correct reference for the element tracing method is Menesguen et al. 2006: "A new numerical technique for tracking chemical species in a multisource, coastal ecosystem applied to nitrogen causing *Ulva* blooms in the Bay of Brest (France)". In the Menesguen and Hoch 1997 paper, a more general method for tracking multiplicative properties of model state variables was described which only later in the later paper was applied for element tracing.

Reply: Changed as suggested.

Figure 1: I suggest to change the color scale. Firstly, it guides the reader's focus to the location of the shelf edge only and makes it hard to distinguish topographic features in the tracing region. Secondly, a scale like that is typically used the opposite way, having the darkest shades of blue at the deepest locations, I would recommend to stick to this habit to make it more intuitive for the reader.

Reply: We inverted the color scale in Fig. 1.

L61-62: Instantaneous benthic remineralization is a good choice if (a) sediment biogeochemistry is in a dynamic steady state (carbon accumulation negligible) and (b) the area is so deep that lateral transport of resuspended organic matter does not play a role. Both assumptions seem questionable here, please discuss the possible implications on your model results.

Reply: Indeed, Song et al. (2016; <https://doi.org/10.1016/j.dsr2.2015.04.012>) determined (based on observations) that on average about 45% of the settled organic matter carbon (~14% of primary production) are permanently buried in the sediments of the East China Sea, although with quite some spatial variability. Consequently, simulated sediment O₂ consumption (SOC) may overestimate the observations, which is consistent with our comparison of simulated and observation-based SOC rates. This likely affects simulated near-bottom O₂, but we consider it having only a small effect on the relative contributions of

individual sources to gross O₂ consumption (GOC), as this limitation equally applies to all labelled N sources.

Sediment resuspension may result in a lower riverine contribution near the river mouths, and higher contributions in more distant areas (vice versa for oceanic contribution). However, except for typhoon events, wind speed (and thus resuspension) is generally lower during summer. Song et al. also state that resuspension may particularly play a role in fall when wind speed starts increasing with the change in the monsoon cycle. We will include this in the discussion of the revised manuscript.

We included this discussion in the revised manuscript (part of new Sect. 4.1, lines 236-246).

L75: Please specify which rivers you prescribed, maybe by adding them as dots in Figure 1 or by supplying a table with their mouths' coordinates in the online supplement.

Reply: We added a table with geographical locations of river input cells to the revised supplement (Table S1). This table is referred to at the appropriate locations in the revised main text: lines 77 and 117.

L86: Please state earlier than in the "Discussion" section what motivates the reduced-oxygen scenarios and why you choose a 20% reduction.

Reply: We added a sentence citing the projection by Earth System Models (Bopp et al., 2017) as the motivation for this reduction at the end of Sect. 2.1 (lines 90-94) of the revised manuscript.

L122: The TN concentrations are actually monthly, daily values are only obtained by interpolation, correct? Please also change the caption of Figure 2.

Reply: Yes, river load concentrations for the Changjiang River are monthly data from Global NEWS. Only freshwater discharge is daily. We corrected the figure caption in the revised manuscript; it's been correct in the main text.

Table 1: How is "anoxic area" defined?

Reply: Anoxic area is defined as the region experiencing O₂ concentrations of 0. We added our definition of anoxic area to the caption of Table 1.

Technical corrections

L59: Citation style is wrong here, please use the "citep" command if the reference can be omitted without changing the meaning of the sentence.

Reply: Has been corrected.

L138: A comma is missing after "South of 32°N".

Reply: Has been corrected.

L278: A comma is missing after "e.g."

Reply: We consistently use no comma after “e.g.” (like on the Biogeosciences website (https://www.biogeosciences.net/for_authors/manuscript_preparation.html); “English guidelines and house standards”). Hence, we did not change it.

Review #2 by anonymous referee

This manuscript quantified the contribution of nitrogen from Changjiang and open ocean (Taiwan Strait and Kuroshio) to the hypoxia formation in the East China Sea and proposed the reduction of nitrogen from river as an efficient way to avoid hypoxia. In general, I can follow this manuscript. However, I also found many points needed to clarify before I can recommend its publication.

General comments

1. Do you include the particle organic nitrogen from rivers? On line 61, you mention only dissolved organic matter (DON) but show TN in Fig. 2. If your TN includes particle organic nitrogen, how did you determine the proportion of PON, DON and DIN (NO₃ and NH₄) in your input data of TN?

Reply: Yes, the river forcing includes information for small and large detritus (=PON), DON, NO₃ and NH₄ (=DIN). However, actual forcing data is only available for NO₃ and NH₄ (from Global NEWS). Therefore, constant concentrations were applied to small and large detritus and DON for all river inputs. We included these values in the revised model description (lines 81/82).

2. Consumption of oxygen by sediment is an important factor affects formation of hypoxia. What is your sediment condition? There is only one sentence (line 62) saying it but it is not enough.

Reply: The statement on line 62 implies that all organic material that sinks to the seafloor is remineralized immediately, with a fraction of 75% being lost to dinitrogen via benthic denitrification (Fennel et al., 2006; <https://doi.org/10.1029/2005GB002456>). Sediment O₂ consumption is proportional to the release of ammonium from benthic remineralization. We expanded the description of the benthic remineralization in the revised model description (lines 61-65) and added a discussion comparing simulated benthic fluxes with literature values and describing its potential impacts on the model results (part of new section 4.1, lines 236-240).

3. You mention the importance of winds in the interannual variations. However, the change of wind speed in Fig. 5 is very small (<2 m/s?). Would you like to present more evidences for the processes related to winds? For example, you mentioned changes in flow field and turbulence but did not show any figures for these changes.

Reply: In terms of absolute numbers, the year-to-year differences in wind speed are indeed relatively small (1-3 m/s). However, considering the discussed events, e.g. September 2008 vs. 2013 and June 2013, it can be seen that the relative change is quite significant as absolute wind speed does not exceed 4 m/s (during these events). In the supplement (Fig. S5;

previously Fig. S2), we provide time series of monthly averaged potential energy anomaly (PEA; a measure for water column stability) over water depth D, which implicitly reflects changes in turbulence as vertical mixing is reduced under more stable conditions. This is discussed on lines X-Y. Along with the PEA/D time series, we show time series of freshwater thickness associated with the Changjiang River discharge. We use freshwater thickness as a measure of the total amount of Changjiang freshwater in the top 25 m of the water column. Changes in freshwater thickness can only result from changes in lateral transport and in discharge from the Changjiang. However, the discharge is quite similar in the first half of 2008 and 2013 (see Fig. 2), thus differences in freshwater thickness between the two years need to be due to differences in transport of freshwater from the Changjiang to the southern analysis region. In addition, changes in freshwater thickness and PEA/D (Fig. S5) clearly coincide with anomalous wind events (Fig. 5). We believe that this PEA/D time series addresses the Reviewer's point about the effect on stratification/turbulence. Furthermore, we added Sect. S6 and Fig. S6 to the revised supplement, illustrating the differences in the surface current fields during June and October of 2008 and 2013 in relation to the year-to-year differences in the wind field (Fig. 5) during these two months. The figure shows how strength and direction of the coastal current are affected by the differences in the wind field between both years. We added a reference to Fig. S6 on lines 190/191 and 195-198 of the revised main text.

4. You emphasized the importance of Changjiang in this study. However, you actually did not consider the interannual variations in the Taiwan Strait and Kuroshio region because you used a nudging to climatology there. The same thing also occurs for the nitrogen from Yellow Sea. Therefore, your conclusion is not fair.

Reply: It is correct, that we do not fully resolve interannual variations in the nitrogen supply from the oceanic sources due to the nudging of nitrate concentrations to a climatology. However, the nutrient supply from the Kuroshio occurs primarily in the subsurface, with open-ocean subsurface concentrations showing significantly lower absolute values (e.g. Liu et al., 2016; <http://dx.doi.org/10.1016/j.jmarsys.2015.05.010>) and lower variability than coastal waters with river influence. Therefore, variations in volume transport of Kuroshio intrusions are likely the main cause for interannual variations in nutrient supply from the Kuroshio. These are resolved by the model. Similarly, nitrogen concentrations in Taiwan Strait (e.g. Chen et al., 2004; <https://doi.org/10.1016/j.marchem.2004.01.006>) are significantly lower than in the river inputs (by factor 10 to 100). Therefore, we consider the effect of interannual variability in nitrogen levels in the oceanic sources small compared to the variability in the river loads.

We added this discussion to the new discussion section on model validation and study limitations (Sect. 4.1, lines 247-254)

5. What is background for reduction of O₂ in the open ocean by 20%? It is better for you to check the papers for DO change at 137E line for some evidences.

Reply: This 20% reduction corresponds to the reduction in subsurface O₂ levels in the northeast Pacific projected by Earth System models (Bopp et al., 2017). We are particularly interested in potential future changes in the O₂ conditions off the Changjiang. We therefore base our scenario on these future projections rather than observations of past changes.

We included the motivation for the 20% reduction of open-ocean O₂ in the revised scenario description (Sect. 2.1, lines 90-94)

6. I did not find figures showing interannual and seasonal variations in spatial variations of bottom DO concentration from your model. Apparently, they are important to your model validation because you can find some observations showing such figures. Without a serious validation of model results, no people in China can follow your suggestion on reduction of nitrogen input by 50%.

Reply: This model-data comparison is provided in the companion paper of Zhang et al. in this same Special Issue (<https://www.biogeosciences-discuss.net/bg-2019-341/>; Fig. 3). We consider it redundant providing the same analysis in this manuscript.

However, we included a qualitative discussion of model-data/literature agreement of observed hypoxic areas in the new discussion section 4.1 of the revised manuscript.

We like to stress that the 50% reduction scenario is only a single model realization and does not suffice to make actual recommendations. We ran this scenario to obtain a first insight into how the system may respond to nitrogen load reductions. The 50% reduction was chosen in analogy to Zhou et al. (2017; <https://doi.org/10.1016/j.marchem.2017.07.006>) who did not consider sediment O₂ consumption in their model, thus missing relevant parts of the system. This is discussed on lines X-Y (previously lines 267-270). As we only ran a single reduction scenario, we are fully aware that we are not in the position of making an actual recommendation and we do not mean to be prescriptive in any way.

Our statement about the potential impact of river load reductions on hypoxia reads as follows in the original version of the manuscript:

“Our analysis of the changes in hypoxic area and hypoxic exposure under reduced Changjiang River N loads (see Fig. 6 and Table 1) underlines the high potential of riverine N load reductions to mitigate hypoxia.” (lines 263-264)

We rephrased it to (change indicated in bold):

“Our analysis of the changes in hypoxic area and hypoxic exposure under reduced Changjiang River N loads (see Fig. 6 and Table 1) **suggests a** high potential of riverine N load reductions to mitigate hypoxia.” (lines 312-313)

Specific comments

Line 29-31: This statement is not correct.

Reply: We rephrased the last part of the sentence to: “with strong southwestward winds in winter and weak northwestward winds in summer supporting stronger northward water mass transport in summer than in winter.” (lines 29-31)

Line 74: please use full spell for ‘FW’.

Reply: “FW” is first introduced on line 20. After that we consistently use “FW” instead of “freshwater”. Therefore, we did not change it.

Line 84-86: “. . .the initial and open-boundary O₂ concentrations were reduced by 20% throughout the water column in regions deeper than 200 m. . .” How much O₂ reduction from the Kuroshio boundary or Taiwan Strait boundary?

Reply: We only reduced the O₂ levels at the open boundaries of the model domain (see Fig. 1 in the manuscript) in regions deeper than 200 m. This means that the inflow of O₂ into the model domain (not the tracing domain) is reduced by 20%. Changes in the O₂ transports in the interior of the model domain (incl. the Kuroshio boundary) can deviate from this reduction due to the internal dynamics.

We expanded the description on what the change in the open-boundary conditions means for the O₂ transports into the model domain in the revised manuscript (Section 2.1, lines 90-99).

Line 110: “. . .Minjiang, Hanjiang and Oujiang Rivers; grouped into one source. . .” You mean Hanjiang River or Qiantangjiang River? In Figure 1, Hanjiang River is not inside the tracing region. How did you trace the N of it?

Reply: We accidentally put a wrong river name, it has to be “Qiantangjiang River”, which we corrected in the revised manuscript (lines 116/117) .

Line 112: What is your evidence for that the tracer cannot reenter the tracing region?

Reply: This is owed to the tracing setup, which does not keep track of the origin of a tracer once it leaves the tracing region. In reality, nutrients could be recirculated into/re-enter the region.

We added text clarifying this to the revised methods section 2.2 (lines 118-120).

Line115: “... To spin up the tracing, we first re-ran year 2006 three times. For the first iteration, all N mass already in the system was attributed to the small rivers.” What’s the purpose of doing this?

Reply: This is done to spin up the model (it is common practice to do so). Note that we do not have information on the actual distributions of nitrogen from the different sources in the region. Therefore, we have to start from an arbitrary distribution for which all nitrogen tracers are attributed to the small rivers (any other of the traced sources would be equally good). We then run the tracing multiple times (3 times in this case) with the same forcing until we achieve a statistical steady state meaning that the distributions of tracers associated with the different sources do not change between December 31 of two subsequent iterations. At this point the model is considered as spun up. This way we make sure that our results are not affected by the arbitrary initial distributions.

We rewrote the last paragraph of Sect. 2.2 in the revised manuscript, hoping that it is more clear now (lines 122-128).

Line125: Figure 2. In 2009, 2011, 2013, the Changjiang discharge and TN concentration seem to have the similar trend, but 2010 and 2012 the opposite. Why does this happen?

Reply: This is a good question, to which we don’t have a definitive answer to. We also note that this question is related to hydrology and thus is well outside the intended scope of the manuscript and our core area of expertise. If we had to speculate, we’d say that to some extent, this could be a result of combining information from two different sources (Global

NEWS for nitrogen concentrations, Datong gauge measurements for discharge). However, more likely this relates to the strong river floods in 2010 and 2012 (indicated by the much higher discharge peaks in both years compared to the other years). We could not find literature explaining this in more detail and emphasize again that it is outside of our field of expertise and outside of the intended scope of this manuscript.

Line 135: do you have any data to verify the GOC given here? Supplement: what is your purpose to show PEA/D not PEA itself?

Reply: We do not have data for GOC but we included a comparison of simulated sediment O₂ consumption with observation-based estimates in the discussion (new Sect. 4.1, lines 229-232).

PEA increases with increasing water depth, which would give stronger weight to deeper regions within the analysis regions. To avoid this, we show PEA/D accounting for this spatial variability of water depth. We added a statement on this to the revised supplement section S5 (page 6, lines 17-20).

Quantifying the contributions of riverine vs. oceanic nitrogen to hypoxia in the East China Sea

Fabian Große^{1,2}, Katja Fennel¹, Haiyan Zhang^{1,3}, and Arnaud Laurent¹

¹Department of Oceanography, Dalhousie University, Halifax, NS, Canada

²Department of Mathematics and Statistics, University of Strathclyde, Glasgow, United Kingdom

³School of Marine Science and Technology, Tianjin University, Tianjin, China

Correspondence: Fabian Große (fabian.grosse@dal.ca)

Abstract. In the East China Sea, hypoxia (oxygen $\leq 62.5 \text{ mmol m}^{-3}$) is frequently observed off the Changjiang (or Yangtze) River estuary covering up to about 15,000 km². The Changjiang River is a major contributor to hypoxia formation because it discharges large amounts of freshwater and nutrients into the region. However, modelling and observational studies have suggested that intrusions of nutrient-rich oceanic water from the Kuroshio Current also contribute to hypoxia formation. The relative contributions of riverine versus oceanic nutrient sources to hypoxia have not been estimated before. Here, we combine a three-dimensional, physical-biogeochemical model with an element tracing method to quantify the relative contributions of nitrogen from different riverine and oceanic sources to hypoxia formation during 2008–2013. Our results suggest that the hypoxic region north of 30 °N is dominated by Changjiang River inputs, with its nitrogen loads supporting 74% of oxygen consumption. South of 30 °N, oceanic nitrogen sources become more important supporting 39% of oxygen consumption during the hypoxic season, but the Changjiang River remains the main control of hypoxia formation also in this region. Model scenarios with reduced Changjiang River nitrogen loads and reduced open-ocean oxygen levels suggest that nitrogen load reductions can significantly reduce hypoxia in the East China Sea and counteract a potential future decline in oxygen supply from the open ocean into the region.

Copyright statement. TEXT

1 Introduction

In the East China Sea (ECS), hypoxic conditions (i.e. dissolved oxygen (O₂) concentrations $\leq 62.5 \text{ mmol m}^{-3}$) are frequently observed off the Changjiang River (or Yangtze) Estuary covering up to about 15,000 km² (Li et al., 2002; Zhu et al., 2017). Hypoxia was first reported in 1959 (Zhu et al., 2011), and a significant increase in its spatial extent has been observed since the 1980s (Li et al., 2011; Wang, 2009; Wang et al., 2015; Zhu et al., 2011). The Changjiang River is the fifth largest river in the world in terms of freshwater (FW) discharge ($9 \times 10^{11} \text{ m}^{-3} \text{ y}^{-1}$) and its nutrient concentrations are comparable to other strongly anthropogenically affected rivers (Liu et al., 2003). The observed increase in hypoxic area since the 1980s has been

attributed to elevated nutrient loads due to fertilizer use in the Changjiang watershed (Siswanto et al., 2008; Wu et al., 2019; Yan et al., 2003).

25 Various studies have suggested that oceanic nutrients also play a role in hypoxia formation in the ECS (Chi et al., 2017; Li et al., 2002; Wang et al., 2018; Zhou et al., 2017b, 2018; Zhu et al., 2011). The importance of oceanic nutrient supply distinguishes hypoxia in the ECS from the otherwise comparable situation in the northern Gulf of Mexico (NGoM), where a similar spatial extent of hypoxic conditions is fueled by freshwater and anthropogenic nutrient inputs from a major river, the Mississippi (Fennel and Testa, 2019). Observations in the ECS indicate that south of 30 °N, intrusions of nutrient-rich water from the Kuroshio Current influence the shelf dynamics (Wang et al., 2018; Zhou et al., 2017b, 2018). These intrusions
30 vary seasonally due to the influence of the East Asian monsoon, with ~~weak northward winds in summer and strong southward winds in winter that lead to northward and southward~~ strong southwestward winds in winter and weak northwestward winds in summer supporting stronger northward water mass transport ~~-, respectively in summer than in winter.~~ (Bian et al., 2013).

The complexity of the circulation and importance of different nutrient sources for hypoxia development make this system particularly amenable to model analyses with high spatio-temporal resolution (Fan and Song, 2014; Zhao and Guo, 2011; Zhang et al., same issue; Zheng et al., 2016; Zhou et al., 2017a; Zhang et al., 2018). Fan and Song (2014) used simulated salinity and nutrient distributions to show that Changjiang River inputs are transported southward in winter and northward in summer. Zhao and Guo (2011) and Zhou et al. (2017a) used model sensitivity studies to highlight the role of oceanic nutrient sources on productivity and hypoxia in the ECS, respectively. Zhang et al. (2019) combined a physical-biogeochemical model with an element tracing method (~~e.g. Ménesguen and Hoch, 1997~~) (e.g. Ménesguen et al., 2006) to quantify the relative contributions
40 of different nutrient sources to primary production (PP). They found that riverine nitrogen (N) supports 56% of water column integrated PP in the ECS regions shallower than 50 m. With organic matter degradation being the main sink of O₂ in the subsurface waters of the ECS (Li et al., 2002), this suggests that riverine N also dominates O₂ consumption. However, a quantification of the relative contributions of riverine versus oceanic nutrient sources to hypoxia has not been available until now.

45 By combining a high-resolution biogeochemical model with this active element tracing method expanded for the quantification of the contributions to O₂ processes (Große et al., 2017, 2019), we provide such an analysis here. We apply the element tracing method to an implementation of the Regional Ocean Modeling System (ROMS; Fennel et al., 2006; Haidvogel et al., 2008) configured for the ECS (Zhang et al., same issue). This allows us to quantify the contributions of N from different riverine and oceanic sources to hypoxia formation in the ECS and analyze year-to-year and seasonal variability in the individual
50 contributions resulting from the East Asian monsoon cycle. In addition to supplying nutrients, the intrusions of open-ocean subsurface waters are relevant to hypoxia by preconditioning O₂ concentrations in the region. Subsurface O₂ has declined over the past decades in the northwest Pacific (Schmidtko et al., 2017) and is projected to continue decreasing in the future (Bopp et al., 2017), which may further exacerbate hypoxia in the region (Qian et al., 2017). We analyze the effect of reduced open-ocean O₂ concentrations on hypoxia under current and reduced N loads from the Changjiang River and compare our
55 results to previous findings for the NGoM's hypoxic zone.

2 Methods

2.1 The physical-biogeochemical model

We used an implementation of ROMS (Haidvogel et al., 2008) for the ECS (Bian et al., 2013). The model covers the region from 116 °E to 134 °E and from 20 °N to 42 °N with a resolution of 1/12 ° (Fig. 1) with 30 terrain-following σ -layers.

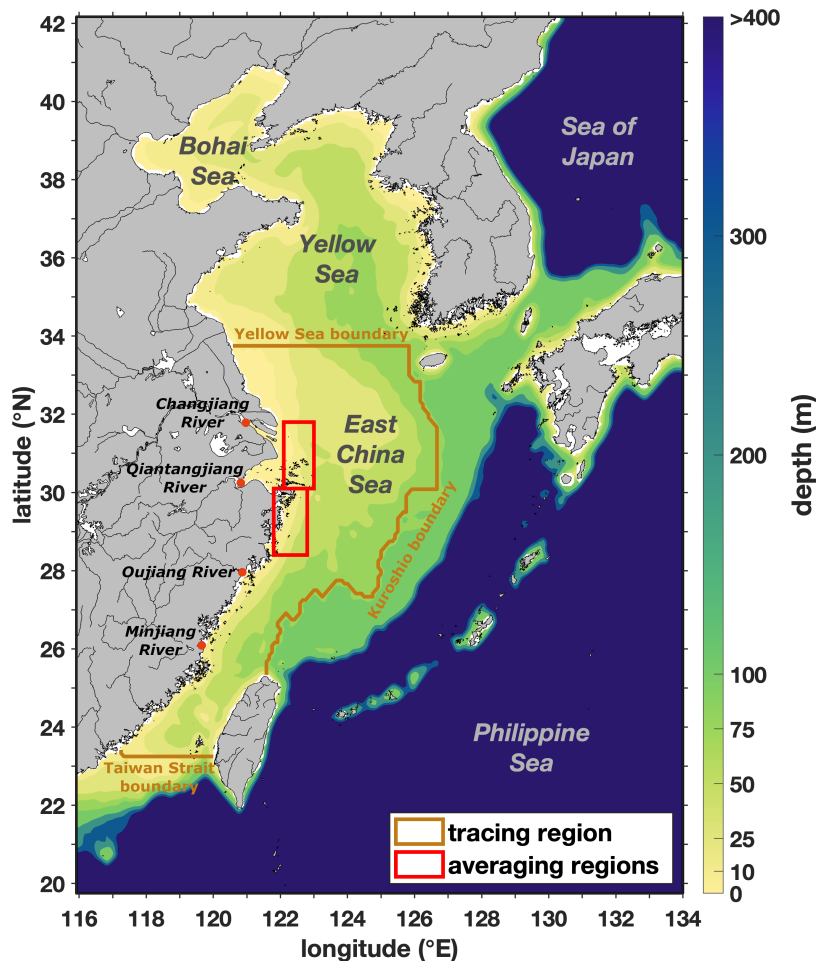


Figure 1. Model domain and bathymetry, with sub-domain used for nitrogen tracing, rivers inside the tracing region, and northern and southern regions used for time series analysis.

60 The biogeochemical component is based on the N-cycle model of Fennel et al. (2006, 2011) but was expanded to include phosphate Laurent et al. (2012), oxygen Fennel et al. (2013) and riverine dissolved organic matter [Yu et al. \(2015\)](#) ([Yu et al., 2015](#)). The model state variables are: nitrate (NO_3^-), ammonium (NH_4^+), phosphate (PO_4^{3-}), one functional group each for phyto- and zooplankton, ~~three groups of detritus (small, large, and riverine dissolved organic matter)~~[small and](#)

[large detritus, riverine dissolved organic matter](#), and dissolved O₂. Instantaneous benthic remineralization was applied at the sediment-water interface (Fennel et al., 2006, 2011). [This implies that all organic matter that sinks to the seafloor is remineralized immediately, with 75% of the deposited N being lost to dinitrogen via benthic denitrification. Sediment O₂ consumption is calculated from the benthic remineralization flux multiplied by a molar ratio of 115:4 between O₂ uptake and release of NH₄⁺.](#) Light attenuation was expanded by including a term dependent on bottom depth (Zhang et al., same issue). For a complete set of model equations we refer the reader to the Appendix of Laurent et al. (2017).

Initial and open boundary conditions for temperature and salinity were derived from World Ocean Atlas 2013 version 2 (WOA13-v2) climatologies (Locarnini et al., 2013; Zweng et al., 2013). Temperature and salinity were nudged weekly toward the climatology using a nudging scale of 120 days. Horizontal velocities and sea surface elevation at the open boundaries are based on the SODA reanalysis (Carton and Giese, 2008). Eight tidal constituents (M₂, S₂, N₂, K₂, K₁, O₁, P₁ and Q₁) are imposed using tidal elevations, and tidal currents are derived from the global tide model of Egbert and Erofeeva (2002). Initial and open boundary conditions for NO₃⁻, PO₄³⁻ and O₂ are also based on WOA13-v2 (Garcia et al., 2013a, b), while small positive values are prescribed for all other biogeochemical variables. In regions deeper than 100 m and in the Yellow Sea north of 34 °N, NO₃⁻ concentrations are nudged toward the climatology using time constants of 7 and 10 days, respectively.

The model was run for the period 2006–2013, with the first two years used as spin-up, and forced by 6-hourly wind stress, surface heat and FW fluxes from the ECMWF ERA-Interim dataset (Dee et al., 2011). Daily FW discharge and nutrient loads for 11 rivers were imposed ([see supplement Table S1 for river locations](#)), with the Changjiang River being by far the largest. Discharge for the Changjiang is obtained from Datong Hydrological Station (<http://www.cjh.com.cn/en/>). Concentrations of NO₃⁻, NH₄⁺ and PO₄³⁻ for the Changjiang River were obtained from the monthly Global NEWS data set (Seitzinger et al., 2005). For the other rivers, FW discharge and nutrient loads were prescribed using climatologies (Liu et al., 2009; Tong et al., 2015; Zhang, 1996). [Due to the lack of data on organic matter loads, river load concentrations of small and large detritus and dissolved organic N were assumed conservatively at 0.5 mmol N m⁻³, 0.2 mmol N m⁻³ and 15 mmol N m⁻³, respectively.](#) The model demonstrates good skill in representing the hydrography and biogeochemistry of the ECS (~~Zhang et al., same issue~~) ([Zhang et al., same issue; Figs. S2–S4](#)) and reproduces the main features of the ECS circulation (~~see supplement Fig-Fig. S1~~). The simulation using this setup is hereafter referred to as the reference simulation.

In addition to the reference simulation, three scenario ~~simulation~~ [simulations](#) were performed: ~~(1) To First, to~~ assess the influence of a reduction in riverine N load on hypoxia, a nutrient reduction scenario was run with 50% smaller N concentrations in the Changjiang River input. All other forcing remained the same. ~~(2) To Second, to~~ investigate the potential effect of reduced open-ocean O₂ supply, a scenario similar to the reference simulation but with reduced O₂ in the open ocean was performed where the initial and open-boundary O₂ concentrations were reduced by 20% throughout the water column in regions deeper than 200 m. ~~(3) The reduced~~ [This implies that simulated O₂ transport into the model domain is reduced by 20% relative to the reference simulation, which corresponds to the changes projected by Earth System Models under an RCP8.5 scenario for the Northwest Pacific Ocean at the end of the 21st century \(Bopp et al., 2017\).](#) Third, the reduced open-ocean O₂ scenario was repeated for reduced river N as in the N reduction scenario.

2.2 Passive freshwater and active nitrogen tracing

Passive dye tracers were used to track FW inputs from the Changjiang River similar to previous ROMS applications (Große et al., 2019; Hetland and Zhang, 2017; Rutherford and Fennel, 2018; Zhang et al., 2010, 2012). The rate of change of the concentration of a passive dye tracer from the i -th source (C_p^i) is described as:

$$\frac{\partial C_p^i}{\partial t} = \nabla \cdot \left(\overline{\overline{D}} \nabla C_p^i \right) \cdot \underline{C_p^i} - \nabla \cdot \left(C_p^i \mathbf{v} \right) + S_{C_p^i}. \quad (1)$$

Here, $\overline{\overline{D}}$ is the second-order diffusion tensor (or diffusivity), \mathbf{v} is the velocity vector, and $S_{C_p^i}$ represents the external dye tracer sources (i.e. riverine FW discharge). The dye tracer was initialized with zero in the entire model domain. Changjiang FW discharge had a dye tracer concentration of 1 and the dye tracer was used to analyze the influence of FW from the Changjiang River on stratification (i.e. potential energy anomaly; Simpson, 1981).

In addition, we applied an active element tracing method (Große et al., 2017; Ménesguen et al., 2006; Radtke et al., 2012) to quantify the contributions of different N sources to O_2 consumption. For this purpose, each model variable containing N is subdivided into fractions from the different source regions or rivers. The rate of change of a specific source fraction is described as:

$$\frac{\partial C_X^i}{\partial t} = \nabla \cdot \left(\overline{\overline{D}} \nabla C_X^i \right) \cdot \underline{C_X^i} - \nabla \cdot \left(C_X^i \mathbf{v} \right) \cdot \underline{C_X^i} + R_{C_X} \cdot \frac{C_{X_{con}}^i}{C_{X_{con}}}. \quad (2)$$

C_X and C_X^i represent the concentrations of state variable X (e.g. NO_3^-) and its labeled fraction from the i -th source (e.g. NO_3^- from the Changjiang River), respectively. R_{C_X} describes internal and external sources and sinks of X . ~~According to Eq., source-specific processes are calculated as the product of the processes acting on each state variable (e.g. uptake during nitrification) and relative concentration of its source-specific fraction.~~ The index ‘con’ in the source/sink term implies that the relative concentration of the variable consumed by a process is used; e.g. source-specific nitrification is calculated based on the relative concentration of NH_4^+ . ~~For each traced source, one set of equations of the form of~~ In our study, Eq. (2) is applied using the solved diagnostically for N tracers from each traced source using the daily model output for the complete N cycle and the post-processing software of Große et al. (2017), which has been adapted for ROMS (Große et al., 2019).

N tracing is only applied in the region without NO_3^- nudging (see ‘tracing region’ in Fig. 1). Inside this region, we simultaneously traced N from five different sources: the Changjiang River, three other smaller rivers (Minjiang, ~~Hanjiang and Oujiang~~ Oujiang and Qiantangjiang Rivers; grouped into one source; see Table S1), the Taiwan Strait (at the southern boundary of the tracing region), the Kuroshio Current (at the eastern boundary), and the Yellow Sea (at the northern boundary; see Fig. 1). ~~Tracers that leave~~ As all N tracers that enter the tracing region across the Taiwan Strait, Kuroshio or Yellow Sea boundaries are labeled as such, this implies that N tracers leaving the tracing region cannot reenter. This tracer setup is similar to that of Zhang et al. (2019), with the difference that we separate the Changjiang River from smaller rivers and that we do not account for atmospheric nutrient deposition.

We applied the N tracing to the reference simulation. ~~To spin up the tracing, we~~ Since the initial distributions of N tracers from the different sources are not known, we apply a spin-up procedure to the tracing, which provides the initial distributions

130 of the labeled N tracers at the beginning of the analysis period 2008–2013. We first re-ran year 2006 three times. For the first iteration, all N mass already in the system was arbitrarily attributed to the small rivers. ~~Subsequent~~, while subsequent iterations were initialized from the final distribution of the previous ~~year, followed by iteration.~~ Comparison of the final states of two subsequent iterations confirmed that a dynamic steady state of the labeled N tracer distributions was reached after three iterations. We then ran year 2007 as an additional spin-up year. ~~This procedure ensures that the different N mass fractions have~~
135 ~~reached a dynamic steady state and produced realistic~~ to ensure that the spatial distributions at the beginning of ~~the analysis period 2008–2013.~~ 2008 are not affected by re-running year 2006.

3 Results

3.1 Changjiang freshwater discharge and nitrogen concentrations

The Changjiang River is the main source of FW and nutrients in the ECS. Daily time series of its FW discharge and total nitrogen (TN) concentrations are shown in Fig. 2. The FW discharge has a distinct seasonal cycle (highest in summer, lowest in winter) due to the monsoon season with high precipitation in summer (Wang et al., 2008), and significant year-to-year variability. The TN concentrations also show high year-to-year variability.

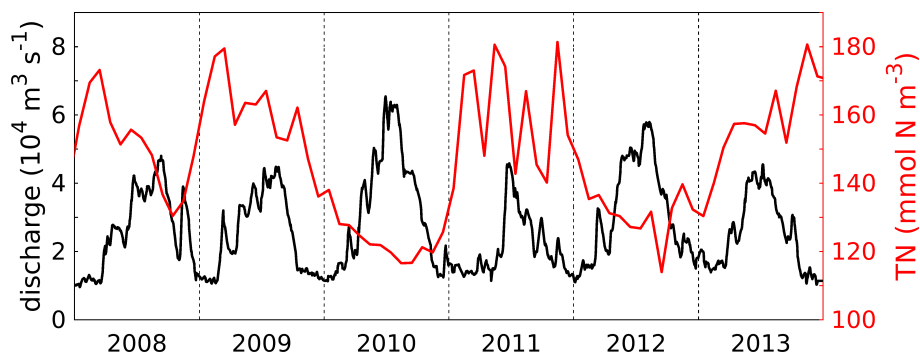


Figure 2. Daily time series of daily freshwater discharge (black, left y-axis) ~~from~~ and monthly total nitrogen (TN) concentration in the Changjiang River (red, right y-axis).

3.2 Spatial patterns in oxygen consumption

We focus our analysis of O_2 dynamics on gross O_2 consumption (GOC), i.e. the sum of sediment O_2 consumption (SOC) and water column respiration (WR; incl. nitrification), and integrate over the 12 deepest pelagic layers (analogous to Zhang et al., same issue). This is reasonable as Zhang et al. show that both SOC and WR are relevant O_2 sinks in the hypoxic bottom boundary layer of the ECS. Hypoxia in the ECS is most pronounced between July and November; we hence focus most of our
145

analyses on this time period. First, we analyze the general spatial patterns in GOC and the relative contributions from riverine and oceanic N sources.

150 Figures 3a and b show maps of GOC and its relative riverine contribution averaged from July to November over the years 2008 to 2013, respectively. GOC is highest (up to $70 \text{ mmol O}_2 \text{ m}^{-2} \text{ d}^{-1}$) in the northern part (30°N to 31°N) of the region typically affected by hypoxia (indicated by the green line). Farther north, GOC is still high (50 to $60 \text{ mmol O}_2 \text{ m}^{-2} \text{ d}^{-1}$), but decreases significantly in the offshore and southward directions with the strongest gradient roughly between 29° , 122.5°E and 31°N , 123°E . The riverine contribution to GOC is highest ($>95\%$) in the coastal regions between 30°N and 32°N and
155 steadily decreases offshore and southward. South of 32°N , the strongest gradient in the riverine contribution corresponds to the maximum gradient in GOC.

Based on the hypoxic area locations simulated in our model and the spatial patterns in GOC and its riverine contribution, we defined two distinct analysis regions (black boxes in Fig. 3): a northern region where GOC is supported mainly by riverine N ($>70\%$) and a southern region where the riverine contribution declines strongly from 75% to 20% in southeastward direction.
160 These regions are used to quantify how the relative contributions of riverine (Changjiang River and smaller rivers) and oceanic N sources (Kuroshio, Taiwan Strait and Yellow Sea) to GOC differ regionally.

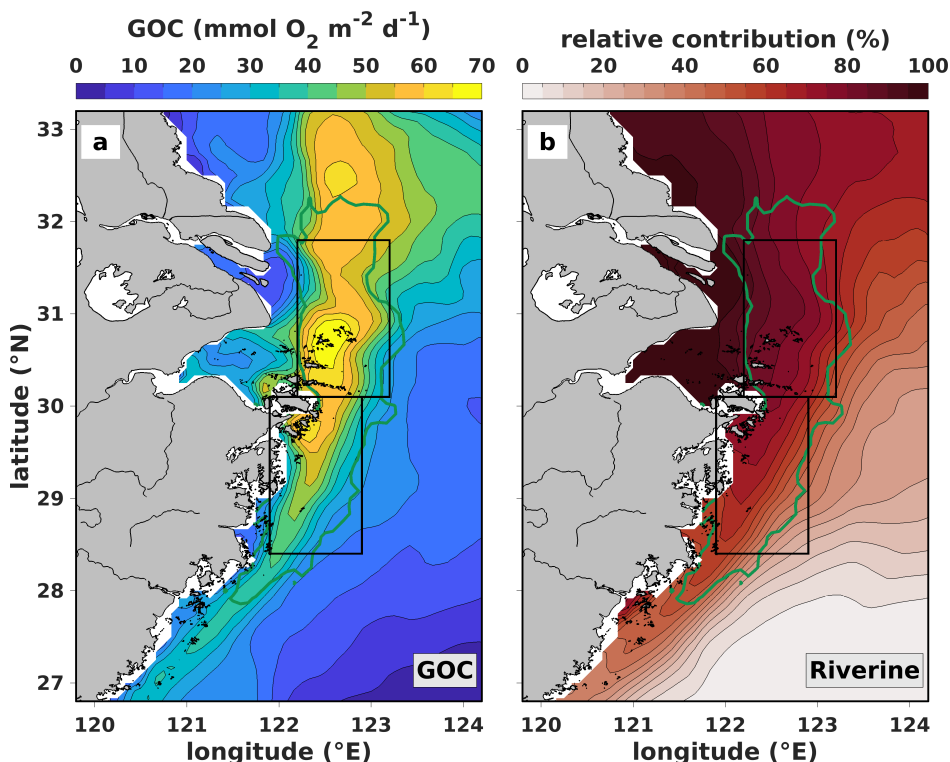


Figure 3. (a) Gross O_2 consumption (GOC) and (b) relative contribution supported by nitrogen from rivers (Changjiang and other rivers) averaged from July to November 2008–2013. Green line: area affected by hypoxia. Boxes: analysis regions used in sections 3.3 and 3.4.

3.3 Year-to-year variability in source-specific oxygen consumption

In order to provide insight in the relative importance of the different N sources for hypoxia formation in the northern and southern hypoxic regions, Fig. 4 shows time series of average source-specific GOC and total hypoxic area from July to November for 2008 to 2013 in both regions. Here, we define total hypoxic area as the area experiencing hypoxia at any time during July to November. The corresponding values of total GOC and the relative contributions of the different sources are provided in Table S1 S2.

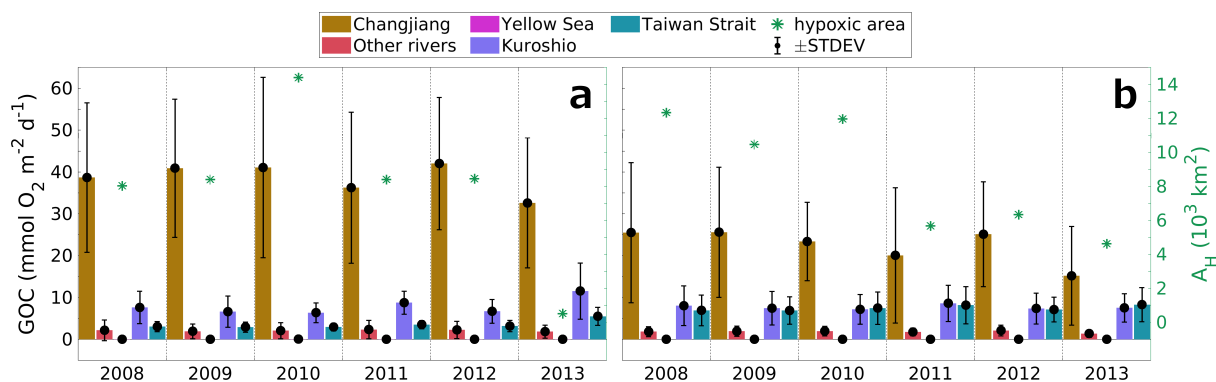


Figure 4. Average source-specific gross O_2 consumption (GOC) and total hypoxic area during July–November of 2008 to 2013 in the (a) northern and (b) southern regions (see Fig. 1). Same legend for both panels.

In the northern region (Fig. 4a), riverine N sources (Changjiang and other rivers) account for $78.0 \pm 5.9\%$ of GOC averaged over 2008–2013, while oceanic sources support only $22.0 \pm 5.9\%$. The Changjiang River constitutes the largest contribution ranging between 63.3% in 2013 and 78.2% in 2010, which are also the years of the smallest and largest hypoxic areas in this time series, respectively. This indicates that the Changjiang River is the main control on O_2 consumption in the northern region.

In the southern region (Fig. 4b), total GOC is about 24% lower than in the northern region, and the riverine contribution is also lower ($61.6 \pm 5.7\%$). The average Changjiang contribution is $56.9 \pm 5.1\%$, while the contributions from the Kuroshio and Taiwan Strait account for $19.5 \pm 2.2\%$ and $18.9 \pm 3.2\%$, respectively. Clearly, N sources other than from the rivers play a role in the southern region.

Interestingly, larger hypoxic areas tend to coincide with high contributions from the Changjiang River and small oceanic contributions (2008–2010), while the tends to be Changjiang is less important in years of small hypoxic areas (2011 and 2013). This suggests that the water mass distribution is an important factor for controlling the extent of hypoxia in the southern region, with a higher Changjiang contribution supporting larger hypoxic areas.

The water mass distribution in the southern region is strongly influenced by large-scale wind patterns, i.e. the East Asian monsoon, and variations in the wind field may affect both seasonal and year-to-year variability in GOC and thus hypoxia. Next,

we analyze the seasonality of source-specific GOC and hypoxic area in relation to the large-scale winds in the southern region in years of small and large hypoxic areas.

3.4 Seasonal cycle of oxygen consumption and hypoxia in the southern region

In the southern region, the largest and smallest hypoxic areas are simulated in 2008 and 2013, respectively. Figure 5 presents 185 monthly time series of source-specific GOC and total hypoxic area for both years. In addition, it shows the 6-year monthly average of the meridional wind speed 10 m above sea level (v_{10}) and the corresponding anomalies for both years.

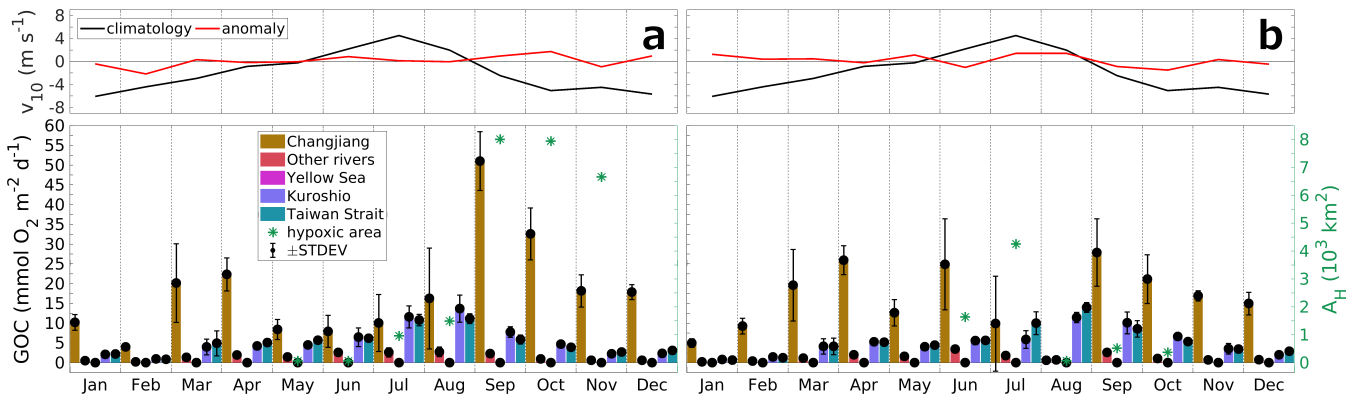


Figure 5. Monthly time series of source-specific contributions to GOC and total hypoxic area (A_H) in the southern region (see Fig. 1) in (a) 2008 (year of largest A_H) and (b) 2013 (smallest A_H), and anomaly of northward wind speed 10 m above sea level (v_{10}) relative to 2008–2013 (‘climatology’) averaged over the ECS (25–33 °N, 119–125 °E). Same legend and axes for both panels.

In general, the Changjiang’s GOC fraction tends to be high in spring (March and April) and in late summer (September). This seasonal pattern is explained by shifts in the dominant wind direction, where the transition from southward to northward winds from March to July results in a northward transport of both the Changjiang River plume and Kuroshio and Taiwan Strait waters increasing the oceanic contribution to GOC. In contrast, the reversal from northward to southward winds in 190 September results in a southward movement of river-influenced water masses. Year-to-year differences in hypoxia, e.g. in June or September/October, result from differences in the Changjiang contribution. The large Changjiang contribution to GOC in September/October 2008 (Fig. 5a) and in June 2013 (Fig. 5b) are followed by large hypoxic areas, while hypoxia almost vanishes in August 2013 when the Changjiang contribution diminishes. These increases (decreases) in the Changjiang 195 contribution also coincide with significant increases (decreases) in FW thickness and thus stratification (see Fig. S2 S5).

The significant year-to-year differences in both the Changjiang contribution to GOC and thus the hypoxic area can be related to year-to-year variability in the wind field and also in FW discharge. The anomalously weak southward winds in September/October of 2008 resulted in a weaker southward coastal current (see Fig. S6). This allowed for a longer presence of Changjiang FW and nutrients in the region stimulating organic matter production and stabilizing vertical density stratification 200 (see Fig. S2 S5). The higher FW discharge in 2008 compared to 2013 (see Fig. 2) also supported stronger stratification. Con-

sequently, the Changjiang contribution to GOC and thus hypoxic area remained large through October and only dropped in November. In June 2013, the anomalously weak northward winds allowed Changjiang water to be transported into the region (see Fig. S6). This caused an increase in GOC and – supported by less wind-induced mixing – stratification, and thus hypoxia. The opposite occurred in July/August of 2013, when anomalously strong northward winds pushed the Changjiang River water northward resulting in a decrease in GOC, stratification and thus hypoxia.

The results from sections 3.3 and 3.4 highlight the importance of Changjiang River nutrients for hypoxia formation in both the northern and the southern regions and suggest that N load reductions in the Changjiang River would mitigate hypoxia also in the southern region. This raises the question how a potential future decline in open-ocean O₂ concentrations would affect hypoxia in the ECS, which is analyzed next.

210 3.5 Potential future changes in hypoxia

The open-ocean water masses travelling to the hypoxic region are not only relevant as N sources but may also act as sources of low-O₂ water, thus preconditioning the region for hypoxia. Consequently, a future decline in subsurface open-ocean O₂ concentrations may exacerbate hypoxia in the ECS. To investigate how reduced open-ocean O₂ concentrations and reduced Changjiang River N loads would affect hypoxia, we performed the scenario simulations described in section 2.1. Figure 6 shows the cumulative hypoxic exposure in the bottom layer from July to November averaged over 2008–2013 for the reference simulation (Fig. 6a), the nutrient reduction scenario with 50% lower Changjiang River N loads (Fig. 6b), the scenario with 20% lower open-ocean O₂ concentrations (Fig. 6c) and the combined scenario with reduced N load and lower open-ocean O₂ (Fig. 6d). Table 1 presents the corresponding changes in different hypoxia metrics between the reference case and the scenarios.

In the reference case (Fig. 6a), hypoxia occurs between 28–32 °N and from the coast to about 123 °E, on average affecting 220 $19.3 \pm 8.1 \times 10^3 \text{ km}^2$. Maximum hypoxic exposure is 28 days in the central parts of the hypoxic region. Hypoxia is still present in the simulation with 50% lower Changjiang River N loads (Fig. 6b), but its areal extent and hypoxic exposure are significantly reduced. Areas affected by continuous hypoxia of more than one and two weeks are reduced by >60%. Hypoxic area increases by about 50% under reduced open-ocean O₂ concentrations (Fig. 6c) and regions affected by continuous hypoxia for more than one and two weeks expand by 86% and 118%, respectively (Table 1).

225 Under reduced open-ocean O₂ and reduced Changjiang River N load (Fig. 6d), simulated changes relative to the reference are still negative, although comparably small (see Table 1). This suggests that N load reductions constitute a potent means to mitigate hypoxia under present conditions and to counteract deterioration of O₂ conditions in ECS due to open-ocean deoxygenation.

4 Discussion

230 4.1 Model validation and study limitations

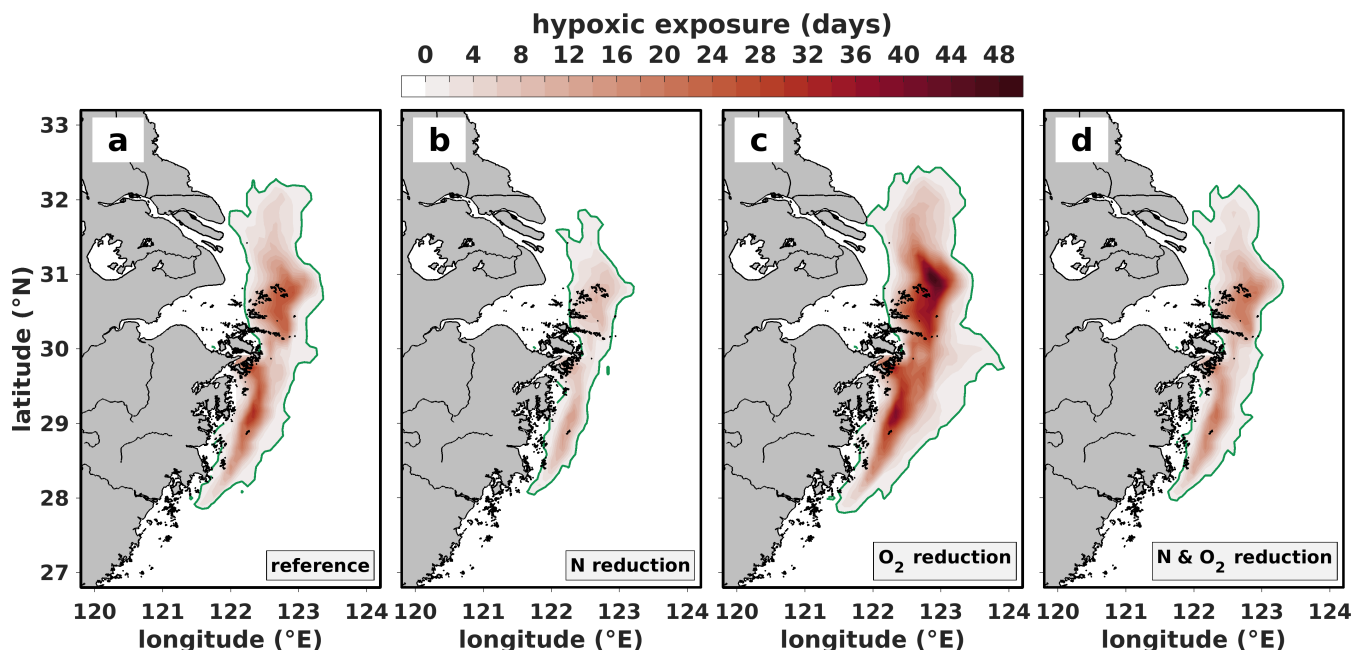


Figure 6. Average cumulative hypoxia during 2008–2013 derived from simulated bottom O_2 concentrations for (a) the reference simulation, (b) the nitrogen reduction scenario, (c) the reference simulation with reduced oceanic O_2 concentrations, and (d) the nitrogen reduction scenario with reduced oceanic O_2 concentrations.

The here applied ROMS model demonstrates good skill in reproducing the hydrography and general circulation of the ECS (Zhang et al., same issue; Fig. S1) and agrees well with both observations (Zhou et al., 2017b, 2018) and other modeling studies (Bian et al., 2013; Guo et al., 2006; Yang et al., 2011, 2012).

235 The simulated spatial distributions of dissolved inorganic nitrogen (DIN) are in agreement with observations of Gao et al. (2015) (see Figs. S2-S4). This, together with the good representation of the circulation, is essential for reliable results of the N tracing. Monthly averaged simulated SOC rates in the analysis regions result in $0.3\text{--}69.8 \text{ mmol } O_2 \text{ m}^{-2} \text{ d}^{-1}$ and are usually within the observed range of $1.7\text{--}62.5 \text{ mmol } O_2 \text{ m}^{-2} \text{ d}^{-1}$ (Song et al., 2016; Zhang et al., 2017). Simulated rates higher than the observed ones only occur in July 2008 and August 2010, which is also the time of year of highest observed rates (Zhang et al., 2017). Zhang et al. (same issue) further show that simulated (daily) hypoxic areas are in agreement with observations, 240 which range between $2,500 \text{ km}^2$ and $15,000 \text{ km}^2$ (Zhu et al., 2017). It should be noted that our values reported for the reference simulation in Table 1 exceed these values as they state the total area affected by hypoxia during each year, while observations are limited to individual months.

245 The instantaneous benthic remineralization (Fennel et al., 2006) used in our model does not take into account sediment burial. Song et al. (2016) estimated that averaged over the ECS shelf about 45% of deposited organic matter (ca. 14% of total primary production) is buried permanently in sediments, although with high spatial variability. This partly explains the slight

Table 1. Hypoxia metrics for the four different cases presented in Fig. 6. A_H : hypoxic area; $A_{H,1w}/A_{H,2w}$: areas with continuous hypoxia for one and two weeks, respectively; A_A : anoxic area (i.e. sum of areas of all grid cells with at least one day of $O_2 = 0$ mmol m⁻³; all in 10³ km²). Values for the reference simulation are total areas. Other values are changes in area (Δ) relative to the reference simulation.

Metric	2008	2009	2010	2011	2012	2013	mean \pm stdev
Reference							
A_H	23.3	20.8	31.0	16.3	18.2	6.4	19.3 \pm 8.1
$A_{H,1w}$	11.2	11.5	18.7	2.8	5.2	0.1	8.2 \pm 6.8
$A_{H,2w}$	4.0	5.7	11.8	0.6	0.9	0.0	3.8 \pm 4.5
A_A	1.8	2.2	3.5	0.1	0.6	0.0	1.4 \pm 1.4
N reduction							
ΔA_H	-11.2	-8.3	-12.4	-14.9	-13.8	-4.9	-10.9 \pm 3.8
$\Delta A_{H,1w}$	-6.9	-7.4	-11.7	-2.8	-4.7	-0.1	-5.6 \pm 4.0
$\Delta A_{H,2w}$	-3.0	-4.4	-8.8	-0.6	-0.9	0.0	-2.9 \pm 3.3
ΔA_A	-1.3	-1.9	-3.5	-0.1	-0.6	0.0	-1.4 \pm 1.3
O ₂ reduction							
ΔA_H	13.6	10.7	9.3	10.6	11.4	9.3	10.8 \pm 1.6
$\Delta A_{H,1w}$	10.4	6.6	7.5	6.5	9.3	2.3	7.1 \pm 5.1
$\Delta A_{H,2w}$	6.8	6.8	7.0	3.0	3.1	0.0	4.5 \pm 2.9
ΔA_A	0.5	0.5	2.8	0.1	0.3	0.0	0.7 \pm 1.1
N and O ₂ reduction							
ΔA_H	-2.3	-2.5	-3.9	-11.8	-5.8	-3.8	-5.0 \pm 3.6
$\Delta A_{H,1w}$	-2.1	-2.5	-4.4	-2.8	-3.2	-0.1	-2.5 \pm 1.4
$\Delta A_{H,2w}$	-1.1	-1.6	-4.1	-0.6	0.0	0.0	-1.4 \pm 1.4
ΔA_A	-0.7	-1.5	-3.2	-0.1	0.0	0.0	-1.0 \pm 1.2

overestimation of SOC rates. However, we consider it having only a small effect on the relative contributions of individual sources to GOC, as this limitation equally applies to all labeled N sources.

250 Sediment resuspension is another process not taken into account in this study. Including this process may result in a lower riverine contribution near the river mouths, and higher contributions in more distant areas (vice versa for oceanic contributions). However, except for typhoon events, wind speed (and thus resuspension) is generally lower during summer (see Fig. 5). Resuspension may play a relevant role in fall when wind speed starts increasing with the change in the monsoon cycle (Song et al., 2016). However, fall defines the end of the hypoxic season. Hence, we consider this effect to be of minor importance to the overall results.

255 It should further be noted that the NO_3^- nudging to a climatology in the off-shelf areas and in the Yellow Sea does not
resolve interannual variability in open-ocean NO_3^- concentrations; however, we believe that these are small. Nutrient supply
from the Kuroshio occurs primarily in the subsurface. With open-ocean subsurface concentrations showing significantly lower
absolute values (e.g. Liu et al., 2016) and lower variability than coastal waters that are directly influenced by river inputs,
neglecting interannual variations in open-ocean NO_3^- concentrations seems justifiable. Variations in volume transport of
260 Kuroshio intrusions are likely the main cause for interannual variations in N supply from the Kuroshio and are resolved by the
model. Similarly, N concentrations in Taiwan Strait (e.g. Chen et al., 2004) are significantly lower than in the river inputs (by
factor 10 to 100).

The diagnostic calculation of the source-specific N fluxes as the product of the fluxes for the non-labeled N tracers and
the ratios of the labeled, source-specific tracers over the non-labeled ones implies that the diffusive fluxes of all labeled N
tracers follow the gradient of the non-labeled (or bulk) N tracers. In reality, diffusive fluxes of matter from N tracers from
265 different sources may be opposed. However, numerical diffusion is known to be higher than background diffusion. Therefore,
we consider the impact on the results to be small.

In summary, the model and N tracing applied here provide a useful basis for a meaningful analysis of our research questions.

4.2 Hypoxia under current environmental conditions

270 Previous observational studies of the hypoxic region off the Changjiang River Estuary have concluded that the regions north
and south of 30°N differ with respect to the nutrient sources contributing to hypoxia formation (Chi et al., 2017; Li et al.,
2002; Zhu et al., 2011). The northern region is considered to be dominated by Changjiang River inputs, while oceanic nutrient
sources are thought to be important in the southern region. Here, we present the first quantification of the relative contribu-
tions of the different nutrient sources to hypoxia formation. Our results show that the riverine contribution to GOC during
275 the hypoxia season (July to November) during 2008–2013 steadily decreases from the northwest to the southeast in the re-
gion typically affected by hypoxia (see Fig. 3). The riverine contribution to GOC dominates the northern region, supporting
 $78.0 \pm 5.9\%$ of GOC ($73.9 \pm 5.4\%$ attributed to Changjiang River), while oceanic N supports only $22.0 \pm 5.9\%$ ($15.2 \pm 3.7\%$
from Kuroshio; see Fig. 4a and Table [S1](#) [S2](#)) confirming that Changjiang River nutrient loads control O_2 consumption and thus
hypoxia formation in the northern region.

280 When considering July–November averages in the southern region, the relative contribution of riverine N to GOC is
 $61.6 \pm 5.7\%$ ($56.9 \pm 5.1\%$ from Changjiang River), while the oceanic contribution is $38.4 \pm 5.7\%$, nearly twice the oceanic
contribution in the northern region, with roughly equal contributions from Kuroshio and Taiwan Strait (see Fig. 4b and Ta-
ble [S1](#) [S2](#)). However, analysis of the seasonal cycles of the source-specific contributions to GOC reveals that hypoxia expands
whenever the Changjiang contribution to GOC increases (see Fig. 5 and Table [S2](#) [S3](#)). This demonstrates that the Changjiang
285 River also is the major factor for hypoxia development in the southern region.

High Changjiang contributions to GOC correspond to high FW thicknesses and thus strong stratification (see Fig. [S2](#) [S5](#)), the
other essential factor for hypoxia formation and maintenance than biological O_2 consumption. In contrast, the hypoxic area is

smaller during periods with high oceanic contributions as a result of reduced GOC and weaker stratification (see Figs. 5 and S2S5). Nevertheless, the relatively low subsurface O₂ concentrations in the oceanic water masses precondition the southern region for hypoxia formation.

Our analyses of the seasonal cycles of GOC and stratification in relation to the large-scale meridional winds further show that the East Asian monsoon and its year-to-year variability result in seasonal and year-to-year variability in the contributions to GOC, in stratification, and thus in hypoxia in the southern region (see Fig. 5). During winter monsoon (September–April), the southward winds transport the Changjiang River plume towards the southern region, where it arrives in August/September supporting the formation of hypoxia. The opposite occurs during summer monsoon (May–August), when the northward winds transport oceanic water masses into the southern region and push the river plume northward out of the southern region.

With respect to year-to-year variability, our analysis further shows that anomalies in the meridional winds during summer and during the transition from summer to winter monsoon (August–October) significantly affect the water mass distribution, and thus GOC and hypoxia on subseasonal scales, especially south of 30°N (see Fig. 5 and Table S2S3). Particularly weak southward winds in September/October of 2008 resulted in a longer presence of the Changjiang River plume in the southern region, increasing stratification and GOC, which in turn caused the formation of the largest hypoxic area in that region during 2008–2013. The opposite occurred in July/August of 2013, when particularly strong northward winds pushed the Changjiang River plume north. This resulted in a drop in GOC and stratification, and in the vanishing of hypoxia, which had started forming in June through early July as anomalously weak northward winds allowed a southward transport of the Changjiang River plume. This is in agreement with Zhang et al. (2018) who simulated similar almost immediate responses of hypoxia to changes in the wind field as a result of the redistribution of Changjiang FW causing changes in stratification. Our study expands on their work by additionally demonstrating the importance of the redistribution of Changjiang nutrients for GOC.

These short-term changes in GOC, stratification and hypoxic area in response to variations in the large-scale winds illustrate the complexity of the region with respect to atmosphere–ocean interaction and their effect on hypoxia. They further highlight the necessity of a high spatio-temporal resolution of both model approaches and observations to understand the causes of hypoxia formation and maintenance in the ECS under current environmental conditions.

In general, our results are in agreement with Zhang et al. (2019) who found that riverine N supports 56% of water column integrated PP (8-year average) in the ECS regions shallower than 50 m, which are most susceptible to hypoxia (see Fig. 3). This confirms the high contribution of Changjiang N to GOC found for our analysis regions. Similarly, the comparably low oceanic contributions, especially in the northern region, are in line with their results. Zhang et al. (2019) also found a relatively high contribution (22%) of atmospheric N to PP suggesting that atmospheric N deposition should be considered in future biogeochemical modeling studies of the ECS.

4.3 Mitigation of hypoxia in the present and future

Our analysis of the changes in hypoxic area and hypoxic exposure under reduced Changjiang River N loads (see Fig. 6 and Table 1) ~~underlines the suggests a~~ high potential of riverine N load reductions to mitigate hypoxia. The simulated average reduction in hypoxic area by 56.5% is almost proportional to the N load reduction of 50% but varies significantly from year

Table 2. Comparison of hypoxia in the northern Gulf of Mexico (NGoM) and the East China Sea (ECS).

Characteristic	NGoM	ECS
Hypoxic area (km ²)	15,000 ¹	15,000 ²
Hypoxic season	May–September ¹	June–November ³
GOC controls (seasonal average)	riverine ≫ oceanic	>30 °N: riverine ≫ oceanic <30 °N: riverine ≈ oceanic
Main riverine source(s)	Mississippi & Atchafalaya	Changjiang
Controls of year-to-year variability	Mississippi & wind field	Changjiang & wind field

¹ Rabalais et al. (2002); ² Li et al. (2002), Zhu et al. (2011, 2017); ³ Wang et al. (2012)

to year (39.9% in 2009 to 91.4% in 2011). Comprehensive further studies are needed to assess the effect of Changjiang River nutrient reductions on hypoxia. In this context, it is important to consider all processes relevant for hypoxia formation. Zhou et al. (2017b) conducted a scenario with 50% lower Changjiang River nutrient loads and found a reduction in hypoxic area by
 325 only about 20%. However, they did not consider SOC, a major sink of O₂ in the ECS (Zhang et al., 2017), which may explain this discrepancy.

Analysis of the scenario where open-ocean O₂ concentrations were 20% lower than at present shows that the reduced lateral supply due to declining open-ocean O₂ concentrations (Bopp et al., 2017) may significantly exacerbate hypoxia in the ECS, indicated by the expansion of both hypoxic and anoxic areas by about 50% (see Fig. 6 and Table 1). However, we further found
 330 that a 50% reduction of the Changjiang River N loads more than compensates for this increase in hypoxia.

The 20% reduction of open-ocean O₂ concentrations that was applied here corresponds to changes in subsurface O₂ of about 30–40 mmol O₂ m⁻³ projected by earth system models (Bopp et al., 2017), but does not consider other climate change effects such as local changes in water temperature or stratification. For instance, an increase in temperature would reduce O₂ solubility, which would worsen O₂ conditions further as shown, e.g. for the NGoM (Laurent et al., 2018). Therefore, more
 335 comprehensive studies on climate change impacts on hypoxia in the ECS are required.

4.4 Comparison with the northern Gulf of Mexico

In the following, we compare the hypoxic zones of the ECS and the NGoM with respect to their sizes and timing, based on observations, and the main sources of O₂ consumption, based on the results of this study and an analogous nutrient tracing study for the NGoM (Große et al., 2019). The key messages of this comparison are summarized in Table 2.

340 The spatial extent of observed hypoxia in the ECS is similar to that in the NGoM, affecting areas on the order of 15,000 km². In the NGoM, hypoxia is frequently observed from May to September when seasonal stratification is strongest due to high riverine freshwater inputs. In the ECS, the hypoxic season starts about one month later in June, with hypoxia forming directly off

the Changjiang River Estuary. Hypoxia can be observed until October/November, though the hypoxic zone moves southward over summer.

345 In the NGoM, riverine nutrients from the Mississippi and Atchafalaya Rivers dominate O_2 consumption. In the ECS, only in the region north of $30^\circ N$ is O_2 consumption dominated by riverine nutrient inputs that almost exclusively originate from the Changjiang River. South of $30^\circ N$, the oceanic contribution to O_2 consumption is comparable to that of riverine nutrients. However, driven by year-to-year variability in the East Asian monsoon, the Changjiang River appears to be the main control of hypoxia formation also in the southern region. Similarly, the Mississippi River in concert with the local wind field seems to
350 be the main control of year-to-year variability in hypoxic area in the NGoM. There, episodic upwelling-favorable winds can result in an offshore transport of Mississippi FW and nutrients leading to a reduction in stratification and O_2 consumption and thus hypoxia (Feng et al., 2014).

5 Conclusions

To our knowledge, this is the first study quantifying the relative contributions of individual riverine and oceanic nutrient
355 sources on hypoxia formation in ECS using active element tracing. Therefore, it constitutes an important milestone towards the quantification of the contributions of riverine vs. oceanic nutrient sources to hypoxia formation in the ECS.

Our results suggest that N from the Changjiang River is the dominant driver of O_2 consumption ($73.9 \pm 5.4\%$) north of $30^\circ N$ under present-day environmental conditions (2008–2013). Contrary to observational insights and despite high contributions of N from Kuroshio and Taiwan Strait to O_2 consumption on seasonal time scales ($19.5 \pm 2.2\%$ and $18.9 \pm 3.2\%$, respectively),
360 the Changjiang River waters are also the main factor for hypoxia formation south of $30^\circ N$.

Our analysis highlights the importance of considering subseasonal time scales for understanding the controls of hypoxia formation and its year-to-year variability in this region. The East Asian monsoon and its associated change in large-scale wind patterns control water mass distribution and thus O_2 consumption and stratification. Year-to-year variability in the intensity of the winds can lead to significant differences in the amount of Changjiang River water in the southern region explaining
365 year-to-year variability in hypoxia.

Reductions in the Changjiang River nutrient loads appear to have a high potential for mitigating hypoxia and to counteract the likely future decline of open-ocean O_2 supplied to the region. However, more comprehensive studies of both the effect of riverine nutrient load reductions and climate change effects are required.

Code and data availability. A modified version of the ROMS source code that facilitates writing of model diagnostics needed by the element
370 tracing software (ETRAC) is available at https://github.com/FabianGrosse/ROMS_3.7_for_ETRAC.

ETRAC is available via <https://github.com/FabianGrosse/ETRAC>. Due to the large data size, ROMS and ETRAC output is freely available upon request from the corresponding author (fabian.grosse@dal.ca).

Competing interests. The authors declare that they have no conflict of interest.

Acknowledgements. All figures in this article were created with MATLAB, benefiting significantly from the toolboxes for TEOS-10 (Mc-
375 Dougall and Barker, 2011), the *cmocean* color schemes (Thyng et al., 2016) and *m_map* (<https://www.eoas.ubc.ca/~rich/map.html>). The
authors of these toolboxes are thankfully acknowledged. The geographical information used for creation of Fig. 1 were obtained from
the Global Self-consistent, Hierarchical, High-resolution Geography Database (GSHHG; <https://www.soest.hawaii.edu/wessel/gshhg/>). We
thank Compute Canada for providing computing resources under the resource allocation project qqh-593-ac. KF acknowledges funding from
the Natural Sciences and Engineering Research Council of Canada (NSERC) Discovery program. Financial support to HZ from the China
380 Scholarship Council (CSC) is gratefully acknowledged. [We thank Hagen Radtke and one anonymous reviewer for their constructive criticism,
which helped to improve this manuscript.](#)

References

- Bian, C., Jiang, W., and Greatbatch, R. J.: An exploratory model study of sediment transport sources and deposits in the Bohai Sea, Yellow Sea, and East China Sea, *J. Geophys. Res.-Oceans*, 118, 5908–5923, <https://doi.org/10.1002/2013JC009116>, 2013.
- 385 Bopp, L., Resplandy, L., Untersee, A., Le Mezo, P., and Kageyama, M.: Ocean (de)oxygenation from the Last Glacial Maximum to the twenty-first century: insights from Earth System models, *Philos. T. Roy. Soc. A*, 375, <https://doi.org/10.1098/rsta.2016.0323>, 2017.
- Carton, J. A. and Giese, B. S.: A Reanalysis of Ocean Climate Using Simple Ocean Data Assimilation (SODA), *Mon. Weather Rev.*, 136, 2999–3017, <https://doi.org/10.1175/2007MWR1978.1>, 2008.
- Chen, C.-T. A., Hsing, L.-Y., Liu, C.-L., and Wang, S.-L.: Degree of nutrient consumption of upwelled water in the Taiwan Strait based on dissolved organic phosphorus or nitrogen, *Mar. Chem.*, 87, 73–86, <https://doi.org/10.1016/j.marchem.2004.01.006>, 2004.
- 390 Chi, L., Song, X., Yuan, Y., Wang, W., Zhou, P., Fan, X., Cao, X., and Yu, Z.: Distribution and key influential factors of dissolved oxygen off the Changjiang River Estuary (CRE) and its adjacent waters in China, *Mar. Pollut. Bull.*, 125, 440–450, <https://doi.org/10.1016/j.marpolbul.2017.09.063>, 2017.
- Dee, D. P., Uppala, S. M., Simmons, A. J., Berrisford, P., Poli, P., Kobayashi, S., Andrae, U., Balmaseda, M. A., Balsamo, G., Bauer, P., 395 Bechtold, P., Beljaars, A. C. M., van de Berg, L., Bidlot, J., Bormann, N., Delsol, C., Dragani, R., Fuentes, M., Geer, A. J., Haimberger, L., Healy, S. B., Hersbach, H., Hólm, E. V., Isaksen, I., Kallberg, P., Köhler, M., Matricardi, M., McNally, A. P., Monge-Sanz, B. M., Morcrette, J.-J., Park, B.-K., Peubey, C., de Rosnay, P., Tavolato, C., Thépaut, J.-N., and Vitart, F.: The ERA-Interim reanalysis: configuration and performance of the data assimilation system, *Q. J. Roy. Meteor. Soc.*, 137, 553–597, <https://doi.org/10.1002/qj.828>, 2011.
- Egbert, G. D. and Erofeeva, S. Y.: Efficient Inverse Modeling of Barotropic Ocean Tides, *J. Atmos. Ocean. Tech.*, 19, 183–204, 400 [https://doi.org/10.1175/1520-0426\(2002\)019<0183:EIMOBO>2.0.CO;2](https://doi.org/10.1175/1520-0426(2002)019<0183:EIMOBO>2.0.CO;2), 2002.
- Fan, W. and Song, J.: A numerical study of the seasonal variations of nutrients in the Changjiang River estuary and its adjacent sea area, *Ecol. Model.*, 291, 69–81, <https://doi.org/10.1016/j.ecolmodel.2014.07.026>, 2014.
- Feng, Y., Fennel, K., Jackson, G. A., DiMarco, S. F., and Hetland, R. D.: A model study of the response of hypoxia to upwelling-favorable wind on the northern Gulf of Mexico shelf, *J. Marine Syst.*, 131, 63–73, <https://doi.org/10.1016/j.jmarsys.2013.11.009>, 2014.
- 405 Fennel, K. and Testa, J. M.: Biogeochemical Controls on Coastal Hypoxia, *Annu. Rev. Mar. Sci.*, 11, 105–130, <https://doi.org/10.1146/annurev-marine-010318-095138>, 2019.
- Fennel, K., Wilkin, J., Levin, J., Moisan, J., O'Reilly, J., and Haidvogel, D.: Nitrogen cycling in the Middle Atlantic Bight: Results from a three-dimensional model and implications for the North Atlantic nitrogen budget, *Global Biogeochem. Cy.*, 20, 1–14, <https://doi.org/10.1029/2005GB002456>, 2006.
- 410 Fennel, K., Hetland, R., Feng, Y., and DiMarco, S.: A coupled physical-biological model of the Northern Gulf of Mexico shelf: model description, validation and analysis of phytoplankton variability, *Biogeosciences*, 8, 1881–1899, <https://doi.org/10.5194/bg-8-1881-2011>, 2011.
- Fennel, K., Hu, J., Laurent, A., Marta-Almeida, M., and Hetland, R.: Sensitivity of hypoxia predictions for the northern Gulf of Mexico to sediment oxygen consumption and model nesting, *J. Geophys. Res.-Oceans*, 118, 990–1002, <https://doi.org/10.1002/jgrc.20077>, 2013.
- 415 Gao, L., Li, D., Ishizaka, J., Zhang, Y., Zong, H., and Guo, L.: Nutrient dynamics across the river-sea interface in the Changjiang (Yangtze River) estuary—East China Sea region, *Limnol. Oceanogr.*, 60, 2207–2221, <https://doi.org/10.1002/lno.10196>, 2015.

- Garcia, H. E., Boyer, T. P., Locarnini, R. A., Antonov, J. I., Mishonov, A. V., Baranova, O. K., Zweng, M. M., Reagan, J. R., Johnson, D. R., and Levitus, S.: World Ocean Atlas 2013. Volume 3: Dissolved oxygen, apparent oxygen utilization, and oxygen saturation, Tech. rep., National Oceanic and Atmospheric Administration (NOAA), Silver Spring, MD, <https://doi.org/10.7289/V5XG9P2W>, 2013a.
- 420 Garcia, H. E., Locarnini, R. A., Boyer, T. P., Antonov, J. I., Baranova, O. K., Zweng, M. M., Reagan, J. R., Johnson, D. R., Mishonov, A. V., and Levitus, S.: World Ocean Atlas 2013. Volume 4: Dissolved inorganic nutrients (phosphate, nitrate, silicate), Tech. rep., National Oceanic and Atmospheric Administration (NOAA), Silver Spring, MD, <https://doi.org/10.7289/V5J67DWD>, 2013b.
- Große, F., Kreuz, M., Lenhart, H.-J., Pätsch, J., and Pohlmann, T.: A Novel Modeling Approach to Quantify the Influence of Nitrogen Inputs on the Oxygen Dynamics of the North Sea, *Front. Mar. Sci.*, 4, 383, <https://doi.org/10.3389/fmars.2017.00383>, 2017.
- 425 Große, F., Fennel, K., and Laurent, A.: Quantifying the Relative Importance of Riverine and Open-Ocean Nitrogen Sources for Hypoxia Formation in the Northern Gulf of Mexico, *J. Geophys. Res.-Oceans*, <https://doi.org/10.1029/2019JC015230>, 2019.
- Guo, X., Miyazawa, Y., and Yamagata, T.: The Kuroshio onshore intrusion along the shelf break of the East China Sea: The origin of the Tsushima Warm Current, *J. Phys. Oceanogr.*, 36, 2205–2231, <https://doi.org/10.1175/JPO2976.1>, 2006.
- Haidvogel, D. B., Arango, H., Budgell, W. P., Cornuelle, B. D., Curchitser, E., Di Lorenzo, E., Fennel, K., Geyer, W. R., Hermann, A. J., Lanerolle, L., Levin, J., McWilliams, J. C., Miller, A. J., Moore, A. M., Powell, T. M., Shchepetkin, A. F., Sherwood, C. R., Signell, R. P., Warner, J. C., and Wilkin, J.: Ocean forecasting in terrain-following coordinates: Formulation and skill assessment of the Regional Ocean Modeling System, *J. Comput. Phys.*, 227, 3595–3624, <https://doi.org/10.1016/j.jcp.2007.06.016>, 2008.
- 430 Hetland, R. D. and Zhang, X.: Interannual Variation in Stratification over the Texas–Louisiana Continental Shelf and Effects on Seasonal Hypoxia, in: *Modeling Coastal Hypoxia*, edited by Dubravko, J., Rose, K. A., Hetland, R. D., and Fennel, K., pp. 49–60, Springer, https://doi.org/10.1007/978-3-319-54571-4_3, 2017.
- 435 Laurent, A., Fennel, K., Hu, J., and Hetland, R.: Simulating the effects of phosphorus limitation in the Mississippi and Atchafalaya River plumes, *Biogeosciences*, 9, 4707–4723, <https://doi.org/10.5194/bg-9-4707-2012>, 2012.
- Laurent, A., Fennel, K., Cai, W.-J., Huang, W.-J., Barbero, L., and Wanninkhof, R.: Eutrophication-induced acidification of coastal waters in the northern Gulf of Mexico: Insights into origin and processes from a coupled physical-biogeochemical model, *Geophys. Res. Lett.*, 44, 946–956, <https://doi.org/10.1002/2016GL071881>, 2017.
- 440 Laurent, A., Fennel, K., Ko, D. S., and Lehrter, J.: Climate Change Projected to Exacerbate Impacts of Coastal Eutrophication in the Northern Gulf of Mexico, *J. Geophys. Res.-Oceans*, 123, 3408–3426, <https://doi.org/10.1002/2017JC013583>, 2018.
- Li, D., Zhang, J., Huang, D., Wu, Y., and Liang, J.: Oxygen depletion off the Changjiang (Yangtze River) estuary, *Sci. China Ser. D*, 45, 1137–1146, <https://doi.org/10.1360/02yd9110>, 2002.
- 445 Li, X., Bianchi, T., Yang, Z., Osterman, L. E., Allison, M. E., DiMarco, S. F., and Yang, H.: Historical trends of hypoxia in Changjiang River estuary: Applications of chemical biomarkers and microfossils, *J. Marine Syst.*, 86, 57–68, <https://doi.org/10.1016/j.jmarsys.2011.02.003>, 2011.
- Liu, S. M., Zhang, J., Chen, H. T., Wu, Y., Xiong, H., and Zhang, Z. F.: Nutrients in the Changjiang and its tributaries, *Biogeochemistry*, 62, 1–18, <https://doi.org/10.1023/A:1021162214304>, 2003.
- 450 Liu, S. M., Hong, G.-H., Zhang, J., Ye, X. W., and Jiang, X. L.: Nutrient budgets for large Chinese estuaries, *Biogeosciences*, 6, 2245–2263, <https://doi.org/10.5194/bg-6-2245-2009>, 2009.
- Liu, S. M., Qi, X. H., Li, X., Ye, H. R., Wu, Y., Ren, J. L., Zhang, J., and Xu, W. Y.: Nutrient dynamics from the Changjiang (Yangtze River) estuary to the East China Sea, *J. Marine Syst.*, 154, 15–27, <https://doi.org/10.1016/j.jmarsys.2015.05.010>, 2016.

- Locarnini, R. A., Mishonov, A. V., Antonov, J. I., Boyer, T. P., Garcia, H. E., Baranova, O. K., Zweng, M. M., Paver, C. R., Reagan, J. R.,
455 Johnson, D. R., Hamilton, M., Seidov, D., and Levitus, S.: World Ocean Atlas 2013. Volume 1: Temperature, Tech. rep., National Oceanic
and Atmospheric Administration (NOAA), Silver Spring, MD, <https://doi.org/10.7289/V55X26VD>, 2013.
- McDougall, T. J. and Barker, P. M.: Getting started with TEOS-10 and the Gibbs Seawater (GSW) oceanographic toolbox, Tech. rep.,
SCOR/IAPSO, http://www.teos-10.org/pubs/gsw/v3_04/pdf/Getting_Started.pdf, 2011.
- Ménesguen, A. and Hoch, T.: Modelling the biogeochemical cycles of elements limiting primary production in the English Channel. I. Role
460 of thermohaline stratification, *Mar. Ecol. Prog. Ser.*, pp. 173–188, <https://doi.org/10.3354/meps146173>, 1997.
- Ménesguen, A., Cugier, P., and Leblond, I.: A new numerical technique for tracking chemical species in a multi-source,
coastal ecosystem, applied to nitrogen causing *Ulva* blooms in the Bay of Brest (France), *Limnol. Oceanogr.*, 51, 591–601,
https://doi.org/10.4319/lo.2006.51.1_part_2.0591, 2006.
- Qian, W., Dai, M., Xu, M., Kao, S.-J., Du, C., Liu, J., Wang, H., Guo, L., and Wang, L.: Non-local drivers of the summer hypoxia in the East
465 China Sea off the Changjiang Estuary, *Estuar. Coast. Shelf S.*, 198, 393–399, <https://doi.org/10.1016/j.ecss.2016.08.032>, 2017.
- Rabalais, N. N., Turner, R. E., and Wiseman Jr., W. J.: Gulf of Mexico Hypoxia, A.K.A. “The Dead Zone”, *Annu. Rev. Ecol. Syst.*, 33,
235–263, <https://doi.org/10.1146/annurev.ecolsys.33.010802.150513>, 2002.
- Radtke, H., Neumann, T., Voss, M., and Fennel, W.: Modeling pathways of riverine nitrogen and phosphorus in the Baltic Sea, *Journal of
Geophysical Research: Oceans*, 117, 1–15, <https://doi.org/10.1029/2012JC008119>, 2012.
- 470 Rutherford, K. and Fennel, K.: Diagnosing transit times on the northwestern North Atlantic continental shelf, *Ocean Sci.*, 14, 1207–1221,
<https://doi.org/10.5194/os-14-1207-2018>, 2018.
- Schmidtko, S., Stramma, L., and Visbeck, M.: Decline in global oceanic oxygen content during the past five decades, *Nature*, 542, 335,
<https://doi.org/10.1038/nature21399>, 2017.
- Seitzinger, S. P., Harrison, J. A., Dumont, E., Beusen, A. H. W., and Bouwman, A. F.: Sources and delivery of carbon, nitrogen, and
475 phosphorus to the coastal zone: An overview of Global Nutrient Export from Watersheds (NEWS) models and their application, *Global
Biogeochem. Cy.*, 19, <https://doi.org/10.1029/2005GB002606>, 2005.
- Simpson, J. H.: The shelf-sea fronts: implications of their existence and behaviour, *Philos. T. Roy. Soc. A*, 302, 531–546,
<https://doi.org/10.1098/rsta.1981.0181>, 1981.
- Siswanto, E., Nakata, H., Matsuoka, Y., Tanaka, K., Kiyomoto, Y., Okamura, K., Zhu, J., and Ishizaka, J.: The long-term freshening and
480 nutrient increases in summer surface water in the northern East China Sea in relation to Changjiang discharge variation, *J. Geophys.
Res.-Oceans*, 113, <https://doi.org/10.1029/2008JC004812>, 2008.
- Song, G., Liu, S., Zhu, Z., Zhai, W., Zhu, C., and Zhang, J.: Sediment oxygen consumption and benthic organic carbon mineralization on the
continental shelves of the East China Sea and the Yellow Sea, *Deep Sea Res. Pt. II*, 124, 53–63, <https://doi.org/10.1016/j.dsr2.2015.04.012>,
2016.
- 485 Thyng, K. M., Greene, C. A., Hetland, R. D., Zimmerle, H. M., and DiMarco, S. F.: True Colors of Oceanography: Guidelines for Effective
and Accurate Colormap Selection, *Oceanography*, 29, <https://doi.org/10.5670/oceanog.2016.66>, 2016.
- Tong, Y., Zhao, Y., Zhen, G., Chi, J., Liu, X., Lu, Y., Wang, X., Yao, R., Chen, J., and Zhang, W.: Nutrient loads flowing into coastal waters
from the main rivers of China (2006–2012), *Sci. Rep.*, 5, 16 678, <https://doi.org/10.1038/srep16678>, 2015.
- Wang, B.: Hydromorphological mechanisms leading to hypoxia off the Changjiang estuary, *Mar. Environ. Res.*, 67, 53–58,
490 <https://doi.org/10.1016/j.marenvres.2008.11.001>, 2009.

- Wang, B., Wei, Q., Chen, J., and Xie, L.: Annual cycle of hypoxia off the Changjiang (Yangtze River) Estuary, *Mar. Environ. Res.*, 77, 1–5, <https://doi.org/10.1016/j.marenvres.2011.12.007>, 2012.
- Wang, H., Yang, Z., Wang, Y., Saito, Y., and Liu, J. P.: Reconstruction of sediment flux from the Changjiang (Yangtze River) to the sea since the 1860s, *J. Hydrol.*, 349, 318–332, <https://doi.org/10.1016/j.jhydrol.2007.11.005>, 2008.
- 495 Wang, J., Yan, W., Chen, N., Li, X., and Liu, L.: Modeled long-term changes of DIN:DIP ratio in the Changjiang River in relation to Chl- α and DO concentrations in adjacent estuary, *Estuar. Coast. Shelf S.*, 166, 153–160, <https://doi.org/10.1016/j.ecss.2014.11.028>, 2015.
- Wang, W., Yu, Z., Song, X., Yuan, Y., Wu, Z., Zhou, P., and Cao, X.: Intrusion Pattern of the Offshore Kuroshio Branch Current and Its Effects on Nutrient Contributions in the East China Sea, *J. Geophys. Res.-Oceans*, 123, 2116–2128, <https://doi.org/10.1002/2017JC013538>, 2018.
- Wu, G., Cao, W., Wang, F., Su, X., Yan, Y., and Guan, Q.: Riverine nutrient fluxes and environmental effects on China's estuaries, *Sci. Total Environ.*, 661, 130–137, <https://doi.org/10.1016/j.scitotenv.2019.01.120>, 2019.
- 500 Yan, W., Zhang, S., Sun, P., and Seitzinger, S. P.: How do nitrogen inputs to the Changjiang basin impact the Changjiang River nitrate: A temporal analysis for 1968–1997, *Global Biogeochem. Cy.*, 17, 1091, <https://doi.org/10.1029/2002GB002029>, 2003.
- Yang, D., Yin, B., Liu, Z., and Feng, X.: Numerical study of the ocean circulation on the East China Sea shelf and a Kuroshio bottom branch northeast of Taiwan in summer, *J. Geophys. Res.-Oceans*, 116, 1–20, <https://doi.org/10.1029/2010JC006777>, 2011.
- 505 Yang, D., Yin, B., Liu, Z., Bai, T., Qi, J., and Chen, H.: Numerical study on the pattern and origins of Kuroshio branches in the bottom water of southern East China Sea in summer, *J. Geophys. Res.-Oceans*, 117, 1–16, <https://doi.org/10.1029/2011JC007528>, 2012.
- Yu, L., Fennel, K., Laurent, A., Murrell, M. C., and Lehrter, J. C.: Numerical analysis of the primary processes controlling oxygen dynamics on the Louisiana shelf, *Biogeosciences*, 12, 2063–2076, <https://doi.org/10.5194/bg-12-2063-2015>, 2015.
- Zhang, H., Zhao, L., Sun, Y., Wang, J., and Wei, H.: Contribution of sediment oxygen demand to hypoxia development off the Changjiang Estuary, *Estuar. Coast. Shelf S.*, 192, 149–157, <https://doi.org/10.1016/j.ecss.2017.05.006>, 2017.
- 510 Zhang, H., Fennel, K., Laurent, A., and Bian, C.: A numerical model study of the main factors contributing to hypoxia and its sub-seasonal to interannual variability off the Changjiang Estuary, *Biogeosciences Discussions*, same issue.
- Zhang, J.: Nutrient elements in large Chinese estuaries, *Cont. Shelf Res.*, 16, 1023–1045, [https://doi.org/10.1016/0278-4343\(95\)00055-0](https://doi.org/10.1016/0278-4343(95)00055-0), 1996.
- 515 Zhang, J., Guo, X., and Zhao, L.: Tracing external sources of nutrients in the East China Sea and evaluating their contributions to primary production, *Prog. Oceanogr.*, 176, 102 122, <https://doi.org/10.1016/j.pocean.2019.102122>, <http://www.sciencedirect.com/science/article/pii/S0079661118301046>, 2019.
- Zhang, W., Wu, H., and Zhu, Z.: Transient Hypoxia Extent Off Changjiang River Estuary due to Mobile Changjiang River Plume, *J. Geophys. Res.-Oceans*, 123, 9196–9211, <https://doi.org/10.1029/2018JC014596>, 2018.
- 520 Zhang, W. G., Wilkin, J. L., and Schofield, O. M. E.: Simulation of Water Age and Residence Time in New York Bight, *J. Phys. Oceanogr.*, 40, 965–982, <https://doi.org/10.1175/2009JPO4249.1>, 2010.
- Zhang, X., Hetland, R. D., Marta-Almeida, M., and DiMarco, S. F.: A numerical investigation of the Mississippi and Atchafalaya freshwater transport, filling and flushing times on the Texas-Louisiana Shelf, *J. Geophys. Res.-Oceans*, 117, C11 009, <https://doi.org/10.1029/2012JC008108>, 2012.
- 525 Zhao, L. and Guo, X.: Influence of cross-shelf water transport on nutrients and phytoplankton in the East China Sea: a model study, *Ocean Sci.*, 7, 27–43, <https://doi.org/10.5194/os-7-27-2011>, 2011.
- Zheng, J., Gao, S., Liu, G., Wang, H., and Zhu, X.: Modeling the impact of river discharge and wind on the hypoxia off Yangtze Estuary, *Nat. Hazard. Earth Sys.*, 16, 2559–2576, <https://doi.org/10.5194/nhess-16-2559-2016>, 2016.

- Zhou, F., Chai, F., Huang, D., Xue, H., Chen, J., Xiu, P., Xuan, J., Li, J., Zeng, D., Ni, X., and Wang, K.: Investigation of hypoxia off the Changjiang Estuary using a coupled model of ROMS-CoSiNE, *Prog. Oceanogr.*, 159, 237–254, <https://doi.org/10.1016/j.pocean.2017.10.008>, 2017a.
- Zhou, P., Song, X., Yuan, Y., Wang, W., Cao, X., and Yu, Z.: Intrusion pattern of the Kuroshio Subsurface Water onto the East China Sea continental shelf traced by dissolved inorganic iodine species during the spring and autumn of 2014, *Mar. Chem.*, 196, 24–34, <https://doi.org/10.1016/j.marchem.2017.07.006>, 2017b.
- 535 Zhou, P., Song, X., Yuan, Y., Wang, W., Chi, L., Cao, X., and Yu, Z.: Intrusion of the Kuroshio Subsurface Water in the southern East China Sea and its variation in 2014 and 2015 traced by dissolved inorganic iodine species, *Prog. Oceanogr.*, 165, 287–298, <https://doi.org/10.1016/j.pocean.2018.06.011>, 2018.
- Zhu, Z.-Y., Zhang, J., Wu, Y., Zhang, Y.-Y., Lin, J., and Liu, S.-M.: Hypoxia off the Changjiang (Yangtze River) Estuary: oxygen depletion and organic matter decomposition, *Mar. Chem.*, 125, 108–116, <https://doi.org/10.1016/j.marchem.2011.03.005>, 2011.
- 540 Zhu, Z.-Y., Wu, H., Liu, S.-M., Wu, Y., Huang, D.-J., Zhang, J., and Zhang, G.-S.: Hypoxia off the Changjiang (Yangtze River) estuary and in the adjacent East China Sea: Quantitative approaches to estimating the tidal impact and nutrient regeneration, *Mar. Pollut. Bull.*, 125, 103–114, <https://doi.org/10.1016/j.marpolbul.2017.07.029>, 2017.
- Zweng, M. M., Reagan, J. R., Antonov, J. I., Locarnini, R. A., Mishonov, A. V., Boyer, T. P., Garcia, H. E., Baranova, O. K., Johnson, D. R., Seidov, D., Biddle, M. M., and Levitus, S.: *World Ocean Atlas 2013. Volume 2: Salinity*, Tech. rep., National Oceanic and Atmospheric Administration (NOAA), Silver Spring, MD, <https://doi.org/10.7289/V5251G4D>, 2013.
- 545